Estuarine benthic nitrate reduction rates: Potential role of microalgae?

Anniet M. Laverman, Jérôme Morelle, Céline Roose-Amsaleg, A. Pannard

Estuarine benthic nitrate reduction rates: potential role of microalgae?

Anniet M. Laverman[1]*, Jérôme Morelle[1], Céline Roose-Amsaleg[1], Alexandrine Pannard[1]

[1]Univ Rennes 1, CNRS, ECOBIO - UMR 6553, F-35000 Rennes, France

*corresponding author: anniet.laverman@univ-rennes1.fr

Graphical abstract

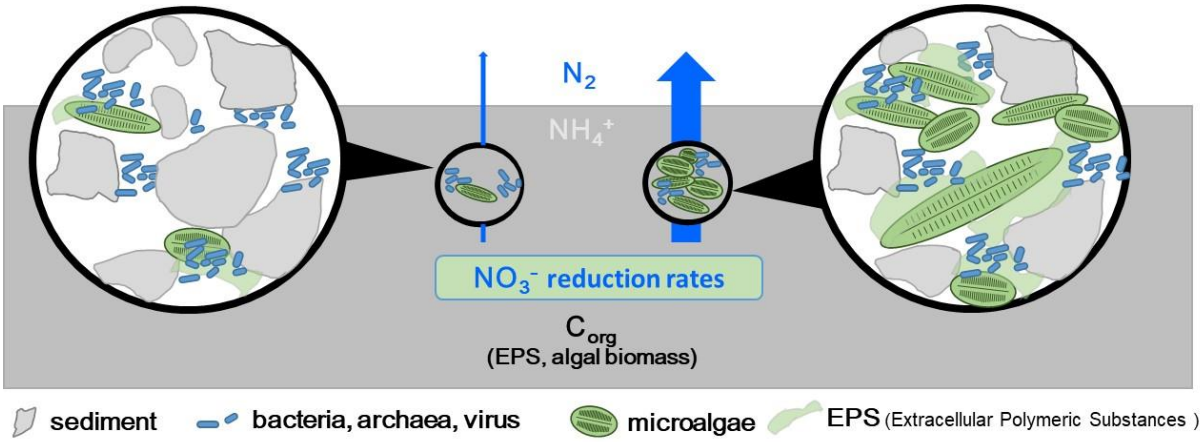

Abstract

The ecological functioning of the Seine estuary is strongly affected by the input of nitrogen, especially in the form of nitrate, which contributes to the eutrophication of the Seine Bight (France). Elimination of nitrate by benthic denitrification in riparian zones or adjacent wetlands could significantly improve the water quality of the Seine estuary. The goal of this study was to investigate the potential for denitrification and the factors affecting these rates. To this end, we measured nitrate reduction and ammonium production rates using flow-through reactors in contrasted sediments collected along the Seine Estuary. Sediment and organic carbon characteristics (organic C, C_{org}:N ratio, bioavailable carbon, extracellular polymeric substances (EPS), chlorophyll *a* and phaeopigments and abundance of nitrogen transforming microorganisms were determined and related to the potential nitrate reduction rates. Nitrate reduction rates showed a large spatial and seasonal variation and showed a significant correlation with sediment phaeopigments, whereas overall microbial activity (ammonium production rates) were highly correlated to chlorophyll *a* and EPS fractions. Surprisingly, bacterial abundance was not correlated to nitrate reduction nor to ammonium production rates. The presence of microalgae appears to be an important driver for nitrate reduction rates in these riparian sediments and seems to have fueled the benthic nitrate reducing activity.

***Key words**:* nitrate reduction, organic carbon quality and quantity, microalgae, estuarine sediments.

1. Introduction

Anthropogenic activity has caused dramatic changes in the global nitrogen cycle. High loads of nitrogen in streams and rivers due to agricultural activity and waste water treatment plant effluents are of concern for the coastal zone due to problems associated with eutrophication (Howarth et al., 1996; Howarth and Marino, 2006). Galloway et al (Galloway et al., 2004) estimated though that 50% of the nitrogen entering streams and rivers may be removed before it reaches the coastal waters.

In the Seine River basin (France), riparian zones have a high potential of nitrate elimination (Thouvenot et al., 2007). The amount of nitrogen supplied to the Seine River by agricultural activity remains high, with little perspective to decrease in the next decades (Garnier et al., 2019). Recurring eutrophication events in the Seine Bay and other sites in the English Channel, including harmful algal blooms are thus expected to persist in the future (Garnier et al., 2019). Therefore, the importance of nitrogen mitigation in the riparian zone is important preventing eutrophication in the Seine Bight (Cugier et al., 2005). Quantifying and identifying factors affecting nitrogen transformation processes in the riparian zone of the Seine are thus crucial in understanding and anticipation of nitrogen elimination.

The main process removing excess nitrate from the environment is microbial mediated denitrification. Denitrification is the microbial respiration of nitrate into reduced nitrogen species, nitrite, nitrous oxide and dinitrogen gas, while oxidizing organic carbon under anoxic conditions (Knowles, 1982; Tiedje et al., 1982). Denitrification is usually limited to the top layers of the sediment where oxygen concentrations are low and nitrate is supplied by the overlaying water. In addition to denitrification, other processes may be responsible for nitrate reduction. Dissimilatory nitrate reduction to ammonium has been shown to play a role, transforming nitrate into ammonium, i.e. without any loss of nitrogen from the system (Tiedje, 1988). Anammox, the anaerobic oxidation of nitrate with ammonium, can eliminate oxidized dissolved nitrogen transforming it into N_2 without requiring the oxidation of organic carbon (Strous et al., 1999; Vandegraaf et al., 1995).

The conditions for denitrification thus require the absence of oxygen, the presence of nitrate as well as the presence of organic carbon (for review see Tiedje et al., 1982). Numerous studies have investigated the relation between organic carbon and denitrification rates in soils and sediments (e.g. Arango et al., 2007; Dodla et al., 2008; Hill and Cardaci, 2004; Sirivedhin and Gray, 2006). In general, the total amount of organic carbon is a poor predictor for denitrification rates (Hill and Cardaci, 2004). Some studies demonstrate a significant positive

correlation between the amount of total organic carbon and denitrifying capacity (Arango et al., 2007; Burford and Bremner, 1975), whereas others show no relationship (Gu et al., 2012; Hill and Cardaci, 2004). This indicates that in addition to the carbon quantity, carbon quality plays a role in the denitrifying capacity in sediments and soils.

Hill and Cardaci (2004) showed that differences in denitrification rates were correlated to anaerobic mineralizable C contents rather than to the total soil organic carbon content. The addition of the same quantity of organic carbon to riparian soils resulted in increased denitrification rates upon watercress and fresh pine needles amendments, whereas significant lower denitrification rates were measured in the presence of senescent needles (Schipper et al., 1994). The role of carbon quality was also demonstrated in coastal wetland soils by a positive correlation of polysaccharide and a negative influence of phenolics on denitrification rates (Dodla et al., 2008).

The impact of carbon quality related to vegetation and its influence on denitrification has been investigated and suggested in several studies (e.g. Bastviken et al., 2007; Fernandes et al., 2016; Groffman et al., 1991). Moreover, algal biomass influences denitrification, as shown by stimulation of denitrification in the presence of senescing green algae (McMillan et al., 2010), and by the increase of denitrifier abundance upon addition of algal biomass in intertidal sediments (Decleyre et al., 2015). Both degradation of algal biomass and the presence of extracellular polymeric substances (EPS) or transparent exopolymeric particles (TEP) secreted by microalgae (Bohorquez et al., 2017; Passow, 2002; Underwood and Paterson, 2003) might also be responsible for this increase in denitrifying activity by providing supplementary sources of anaerobic mineralizable C in sediments. Both terrestrial and aquatic vegetation plays a role in nitrate reduction *via* the supply of labile and available organic carbon during the degradation of suspended organic matter (SOM) and consequently nitrate removal in soils and sediments. Therefore, the objective of this study was to determine the impact of terrestrial and aquatic vegetation on nitrate reduction rates in riparian estuarine sediments. We hypothesized that carbon quality rather than carbon quantity drives nitrate reduction rates in these sediments. To investigate the impact of carbon quality and quantity on nitrate reduction rates, we determined nitrate reduction rates as well as sediment characteristics in four different estuarine sediments collected along the Seine River estuary during three different seasons. We used flow-through reactors to determine the rates under controlled conditions, using intact sediment and thus the resident microbial community and site specific sediment conditions. In addition to total sediment organic carbon (C_{org}), parameters related to organic carbon quality were determined;

the biodegradable organic carbon content (BDOC), %N, C_{org}:N ratio, chlorophyll *a* (chl *a*) and phaeopigments concentrations as well as the EPS fractions (proteins and carbohydrates). In order to determine whether the bacterial abundances were related to the rates and sediment characteristics, bacterial abundances as well as those representing the major nitrogen cycling microbes were enumerated. Nitrate reduction rates were linked to the aforementioned sediment characteristics and the role of intertidal mudflats mitigating as nitrogen sink is discussed.

2. Materials and Methods

2.1 Study sites and sampling

Surface sediments were collected at 4 sites along the Seine River, France, from just upstream of Rouen until the estuary mouth (Figure 1). Sediments were collected at low tide when the sediments were accessible. The most upstream site with near "Saint Etienne du Rouvray" is a riparian wetland (**RW**, 49°22'12.21"N, 1° 7'13.33"E). It is an old river arm of the Seine, which is divided in two by an embankment isolating the river the upstream part. The site corresponds to a closed river arm of the Seine, still connected to the main river and subject to variations in water levels in relation to the tide. The site is dominated by reed and willow. "Grand vase petit vase", near Quevillon (49°25'1.84"N, 0°56'10.45"E), is an artificial wetland (**AW**) that was created for the deposition of dredging material from the Seine. This so called "deposit chamber" is connected to the river artificially. At high tide, the site is filled with water from the Seine River, whereas a valve prevents the water to flow back into the river. "Trou deshayes" (49°27'22.02"N, 0°51'32.98"E), a freshwater mudflat (**FM**), is a site separated from the river by a dike with drains containing valves allowing the evacuation of water towards the river, at the same time preventing inverse flow (from the river to the wetland). This site is fed by runoff from the alluvial plain and is also influenced by the alluvial groundwater table, main vegetation is bullrush. The most downstream site, an intertidal mudflat (**IM**), near the village Petiville (49°25'53.04"N, 0°36'20.87"E), is in direct connection to the Seine River.

Nitrate reduction, nitrite and ammonium production rates and sediment characteristics were determined in June, September 2010 and March 2011. Sediment from the top first cm was collected for experiments, analysis of sediment characteristics and enumeration of the total bacterial and denitrifier abundance. Surface water at each sampling site was collected with a 20

mL syringe, filtered (0.2 µm pore size) and kept at 4° C during transport (less than 6h) and frozen until nutrient analysis (NO_3^-, NO_2^-, NH_4^+).

2.2 Flow-through reactor (FTR) experiments

Nitrate reduction as well as nitrite and ammonium production rates were determined in the top sediment (0-1 cm) using flow-through reactors. The flow-through reactor (FTR) design and the determination of potential rates were extensively described previously (Laverman et al., 2006; Pallud et al., 2007; Pallud and Van Cappellen, 2006; Roychoudhury et al., 1998). Upon collection at low tide, sediments were kept at 4°C until the start of the experiments, which were started within 24 hours.

The sediment in the reactor was supplied with a constant inflow anoxic nitrate solution (5 mM $NaNO_3$) at ambient salinity (NaCl) at a constant flow rate of 4.0±0.2 mL h^{-1} (Q) using a peristaltic pump (Minipuls 3®, Gilson). In these sediments, with a porosity between 0.7 – 0.9 (data not shown), this flowrate has been shown not to influence the potential microbial reaction rates (Pallud et al., 2007). Note that this flowrate does not mimic *in situ* flowrates. The anoxic inflow conditions were achieved by bubbling the solutions for 10 minutes with N_2 gas, kept in a 1 L Schott bottle closed with a HPLC type cap, to ensure gastight conditions during the experiment. The HPLC type cap contains an inlet to flush the solution (closed during the experiment), an outlet that is connected to the peristaltic pump and a pressure in/outlet. The latter is connected to a syringe filled with N_2 to compensate possible under pressure during the experiment and avoiding inflow of air. The reactor outflow solution was sampled at 3 to 4-hour intervals using a fraction collector over a period of 44 to 50 hours. Reactors were run in duplicate in June 2010 and March 2011 (44h), which led to 6 samples per reactor at steady state conditions (20 hours, duplicate reactors n=12). In September 2010 triplicate reactors were run (50h), for FM 1 reactor was clogged and duplicate reactors were taken into account for the rate determinations, steady state rates were determined upon 14 hours at 3h intervals (36 h, duplicate n=24, triplicate n=36).

Nitrate reduction, nitrite, ammonium production rates were calculated by multiplying the flow rate, Q, by the concentration difference of the nitrogen species in the input and output solutions and normalized to gram dry sediment (see for details Laverman et al 2012). All rates are expressed in units of nmol per gram dry sediment per hour. Nitrate reduction rates (NRR) were calculated from the measured difference in nitrate concentration between inflow and

outflow solutions. For the nitrite production rates (NiPR) and ammonium production rates (APR) the inflow concentrations were zero. Note that the rates were determined at constant temperature (20±2°C) under fully anoxic conditions in the laboratory and are thus referred to as potential rates. These rates reflect potential rates of the resident microbial community and sediment organic matter.

2.3 Analytical methods

Nitrate, nitrite and ammonium concentrations were measured colorimetrically with a Nutrient Autoanalyzer 3 (Brann and Luebbe, Thermo Scientific). Sediment organic C and total N contents were determined on freeze-dried samples using a LECO CS 125 CN analyzer. The sediment samples were acidified drop by drop (100 µl) with 2N HCl to remove the inorganic carbon.

The amount of biodegradable fraction of the organic carbon (BDOC) in the sediments was measured using the experimental procedure of Servais et al. (1999). To this end 1 cm^3 of wet sediment was homogenized in a 1 L bottle with 300 mL deionised water and incubated at 21±2 °C. During incubation the batch was intermittently aerated in order to maintain aerobic conditions. Subsamples of 40 mL were collected at the beginning and after 45 days of incubation. They were centrifuged (10 minutes 3000 rpm), the supernatant was transferred to a glass vial and preserved with 12N HCl (80 µL) and kept at 4°C until DOC analysis by high temperature combustion (Shimadzu TOC-5050A analyzer). The solid pellet was freeze dried, grinded, acidified and its C content was measured using a total carbon analyzer (LECO CS 125, EPOC, University Bordeaux 1).

Chlorophyll *a* (Chl *a*) and phaeopigments (Phaeo) concentrations in the sediments were determined according to Lorenzen (1967). The pigments were extracted from 0.5 g of sediment suspended in 10 mL acetone (90%), by continuously rotating (12 rpm) the samples for 12 h in the dark at 4 °C. After centrifugation (4 °C, 2000 *g*, 5 min), fluorescence of the supernatant was measured using a Fluorometer Turner TD-700 before and after acidification (10 µL HCl 0.3 M for 1 mL acetone). Chlorophyll *a* and phaeopigments were then measured using the fluorometric method (Lorenzen, 1967).

Colloidal EPS were extracted from almost 0.5-1 g of dried sediment and placed in 15 mL centrifugation tubes in 5 mL of deionized water (MilliQ). After 1 h of incubation at 35°C under continuous mixing, tubes were centrifuged at 4 °C, 3000 *g* for 10 min. Supernatants containing the EPS were collected in a new centrifugation tube. Low and high molecular weight EPS

(LMW and HMW) were extracted from the supernatants after incubation in ethanol (70% final concentration) for 16 h at − 20 °C. Samples were centrifuged (4 °C, 3000 *g*, 30 min). LMW EPS were collected in the supernatant and HMW EPS were collected in the pellet. The supernatant was decanted into a new tube and both the supernatant and the pellet were dried at 60 °C in a dry bath under air flow (from 6 to 48 h depending on the fraction). The dried samples were resuspended in 5 mL deionized water and stored at − 20 °C for LMW and HMW carbohydrate and protein quantification. Total sugar content was determined using the phenol–sulfuric acid assay with glucose as a standard (Dubois et al., 1956) and protein content was determined using the Bradford assay reagent (Bio-Rad) with bovine serum albumin from Sigma-Aldrich as standard (Bradford 1976). Absorption was read after 30 min with a FlexStation plate reader (Molecular Devices) at 485 nm for carbohydrates and 590 nm for proteins. All results are expressed per gram dry sediment (gds^{-1}).

2.4 Microbial abundance measurements

Fresh sediments were collected at the end of the FTR incubation and stored at -80°C until DNA extraction. Microbial DNA extraction was carried out according to the protocol described in (Griffiths et al., 2000). DNA quality and quantity were determined using a Spectrostar nano (BMG labtech). Quantitative PCRs were conducted with a Roche LC480 thermocycler using different primer sets targeting several groups of microorganisms. The *nosZ* gene of denitrifying bacteria (able to transform N_2O in N_2), by using the nosZ−F (5'−CGYTGTTCMTGGACAGCCAG, (Kloos et al., 2001) and nosZ1622Rb (5'−CGCRASGGCAASAAGGTSCG (Throbäck et al., 2004) primer set. The *nrfA* gene for DNRA (nrfAF2aw 5'CARTGYYGTBGARTA-3', (Welsh et al., 2014) and nrfAR1 5'-WNGGCARTTGRCARTC-3' (Mohan et al., 2004). A region of the *16S rRNA* gene specific to anammox bacteria (A438F 5'-GTC RGG AGT TAD GAA ATG-3' and A684R 5'-ACC AGA AGT TCC ACT CTC-3', (Humbert et al., 2012)). *The 16S rRNA* gene copies were also quantified in order to determine a proxy of the whole bacterial density (given that one genome can contain up to 15 copies of *16S rRNA* genes) using the following primer set: 63f (5'-CAGGCCTAACACATGCAAGTC-3' (Marchesi et al., 1998) and BU16S4 (5'-CTGCTGCCTCCCGTAGG-3', derived from 341F (Muyzer et al., 1993).

Reactions were set up in triplicate; no-template controls in duplicate. Absolute quantification was performed using 5 serial 10-fold dilutions (in duplicate) using: *Pseudomonas*

fluorescens SBW25 for *16S rRNA* or gene calibrators from *Escherichia coli* K12 strain for *nrfA gene* and from *Brocadia sp.* (KJ701283) for anammox *16S rRNA gene* and *Bradyrhizobium japonicum* USDA 110 strain for *nosZ* gene.

The LC480 software delivered melting curve analysis and second derivatives for crossing point (Cp) allowing determination of copy numbers. The detection limit was defined as fluorescent signals with at least 5 Cp below the signal of the no-template controls. All the results are expressed in log copy numbers per gram dry soil (log copies gds^{-1}).

2.5 Statistical methods

To explain patterns of chemical variability in sediment, the sediment characteristics determined at the four stations in March, June and September were investigated using a Principal Component Analysis (PCA), after scaling and reducing the data. All the statistical analyses were performed using Rstudio (R Core Team 2018), and more specifically, the PCA was performed using *factoextra* library implemented in R (Kassambara and Mundt, 2017).

To highlight factors that best explain the reaction rates in the sediment (Nitrate reduction NRR, nitrite production NiPR and ammonium production APR), we used a redundancy analysis (RDA), with a forward selection procedure of the predictors including all chemical variables (Blanchet et al., 2008). The RDA first performs a multivariate multiple linear regression, then a PCA of the fitted values, and lastly a permutation test of the significance by randomly permuting rows and columns. Collinearity between explanatory variables have also been tested. The RDA was performed using *vegan* and *ade4* libraries in R (Borcard et al., 2011).

3. Results

3.1 Site and sediment characteristics

Dissolved nitrogen concentrations in the overlaying water at the sampling sites throughout the different seasons showed a strong spatial variation. Nitrate was generally the dominant form of dissolved nitrogen, with highest values in the riparian wetland (70-400 µM) and values ranging from 0-105 µM in the artificial wetland, 2-200 µM in the freshwater mudflat and 63-140 µM in the intertidal mudflat. Ammonium concentrations were high in the riparian wetland (14-929 µM), intermediate in the freshwater mudflat (11-60 µM) and intertidal mudflat (9.3-30 µM) and low in the artificial mudflat (0.7-4.6 µM). Nitrate concentrations in the channel of the Seine River range between 360 to 500 µM NO_3^- (5 to 7 mg N/L), between 2009 and 2010 at Poses (Garnier et al 2019).

3.1.1 Bacterial abundances

Bacterial abundances were similar (9.2-10.1 log gds^{-1}, Table 1) for the total benthic bacterial community over the different seasons. Denitrifiers represented less than 8% of the benthic bacteria, bacteria involved in DNRA less than 0.8% and bacteria involved in anammox 0.01% when detectable. The most abundant bacteria able to metabolize nitrate or nitrite were always the denitrifiers at all sites with the smallest percentages in the artificial wetland and intertidal mudflat and highest in the riparian wetland and freshwater mudflat (see Table 1)

3.1.2 Total and degradable carbon

The total organic carbon contents showed a large variation between the sites and seasons (Table 2). Lowest organic carbon contents were found for the different seasons in the artificial wetland and intertidal mudflat sediments, varying between 1.2 and 2.8%. The highest levels of total organic carbon were found in the sediments of the freshwater mudflat varying between 4.4 and 5.6 % carbon. Relatively high carbon contents were also found in the riparian wetland sediments, with a large seasonal variation, varying between 2.5-5.7% organic carbon. Most of the sediment C_{org}:N ratios are below 11 (Table 2), except high values obtained in the riparian wetland sediment varying between 31 and 44.

303 The amounts of biodegradable carbon (BDOC) varied between 1 to 13.8 mg C gds^{-1} for
304 the different sampling sites (Table 2). The fractions of BDOC were highest in the freshwater
305 mudflat and riparian wetland ranging from 6 to 14 mg gds^{-1}, lower values were determined for
306 the artificial wetland (1 – 3.3 mg gds^{-1}) and intertidal mudflat (2.4 – 7 mg gds^{-1}). The fraction
307 of biodegradable carbon of the total organic carbon content ranged between 10 to 44% for the
308 different sediments and showed a high seasonal variation (Table 2). For the riparian wetland
309 (16–24%), artificial wetland (9-24%) and the freshwater mudflat (10-27%) the values ranged
310 between 9 and 27%. A larger range of the BDOC fractions was determined in the intertidal
311 mudflat between 11 and 44% with a high fraction of 44% in March.
312
313 **3.1.4 Algae and EPS**
314 Sedimentary chlorophyll *a* and phaeopigment concentrations were highest in the
315 freshwater mudflat sediments, with concentrations of chl *a* between 21 and 124 µg chl*a* gds^{-1}
316 and phaeopigments ranging from 253 till 611 µg chl*a* gds^{-1} (Table 2) The highest values for chl
317 *a* and phaeopigments did not coincide, chl *a* was highest in March, whereas phaeopigments
318 were highest in June. Lowest and least variable levels of chl *a* (3.3- 8.5 µg chl*a* gds^{-1}) and
319 phaeopigments (13 – 48 µg eq chl*a* gds^{-1}) were measured in the sediments of the riparian
320 wetland. The artificial wetland and brackish mudflat sediments contained chl *a* and
321 phaeopigment concentrations between respectively 6.3 to 63 µg chl*a* gds^{-1} and 5.3 to 80 µg chl*a*
322 gds^{-1}.
323 The different fractions of the extracellular polymeric substances (EPS) in the different
324 sediments were dominated by the carbohydrates (ranging between 174 – 313 µg gds^{-1}) with
325 several order of magnitude lower contents of proteins (HMW 0.2 – 8.5 µg gds^{-1}; LMW 0.7 – 7
326 µg gds^{-1}). Regarding the total contents of HMW carbohydrates (Table 2), the highest values
327 were measured in the freshwater mudflat (247-313 µg gds^{-1}) while the lowest values were
328 measured in the intertidal mudflat (174-199 µg gds^{-1}). Highest values were measured in June,
329 except in the artificial wetland. Despite being in the same order of magnitude, LMW
330 carbohydrates values showed lower variation between sites and seasons. The protein EPS
331 contents were highest in the freshwater mudflat sediment (HMW 4.5 – 5.8, LMW 4.2 – 7 µg
332 gds^{-1}) and lowest in the riparian wetland sediment (HMW 0.2 – 1.7, LMW 0.7 – 2.3 µg gds^{-1},
333 see Table 2 for details).
334

335 **Correlations**

336 Principal component analysis of the sediment features revealed spatial and temporal
337 patterns in the sediment characteristics (Figure 2). The first two principal components (PC1 and
338 PC2) explained respectively 51 and 21% of the total variance in the chemical data. The first
339 axis was explained by several correlated parameters: the phaeopigment concentrations (Phaeo)
340 at 13.6%, the LMW protein fraction of the EPS (prot LMW) and the N content both at 12%, the
341 HMW carbohydrate (carb HMW) at 10.4%, the organic carbon (C_{org}) and the log-transformed
342 denitrifying bacterial numbers (LOGnosZ) both at 9.5% (Fig. 2). The biodegradable carbon
343 (BDOC) contents were positively correlated to the C_{org} content (Spearman correlation, r_S=0.68;
344 p = 0.017), while phaeopigments correlated positively with sediment N content (r_S=0.87; p <
345 0.001). The second axis was explained by the C_{org}:N ratio (32%), the BDOC (12.9%), the HMW
346 protein fraction of the EPS (prot HMW; 12.5%). The LOGnosZ, which already contributes to
347 the first axis, contributes at 9.6% to the second axis. The first axis of the PCA is explained by
348 the freshwater mudflat on the left part of the plot, with 31.9%, 22.6% and 16.3% for June,
349 September and March samples respectively (Fig. 2). At the opposite side, the March sample
350 from the artificial wetland explained 10.6% of the first axis. The second axis of the PCA is
351 explained by the March and September samples from the riparian wetland (57.2% and 7.9%
352 respectively) at the top of the plot (Figure 2). Finally, the freshwater mudflat showed high
353 concentrations of Phaeo, C_{org}, LMW protein fraction of the EPS, the HMW carbohydrates (carb
354 HMW), N and LOGnosZ, whatever the sampling date, while the artificial wetland showed high
355 C_{org}:N ratios in March and also in September (Figure 2).
356
357
358 ***3.2 Nitrate reduction and ammonium production rates***

359 Nitrate reduction rates varied among sites and between seasons (Figure 3, SI Table1).
360 Highest nitrate reduction rates were measured in the sediments of the freshwater mudflat,
361 especially in June and September with maximum rates up to 3000 nmol gds^{-1} h^{-1}, with lower
362 rates in March (see Figure 3). Overall, the sediments from the different sites showed seasonal
363 differences of the potential nitrate reduction rates. Lowest rates were found in March, with
364 higher rates in June and September for the sediments from the riparian and artificial wetland
365 and brackish mudflat sediments.

366 The ammonium production rates from the same sediments and seasons under nitrate
367 reducing conditions, show seasonal variations, however not similar to nitrate reduction rates

(Figure 3). The riparian wetland sediment shows low ammonium production rates and little seasonal variation. The artificial wetland sediment showed highest ammonium production in March and low rates in June and September, dissimilar to the nitrate reduction rate dynamics. Highest ammonium production rates were measured from the freshwater mudflat sediments, the site with highest nitrate reduction rates, in March and June and lowest at this site in September. The intertidal mudflat sediments showed highest and most variable ammonium production rates in September and were low in March and June.

To highlight which sediment characteristics explain the microbial reaction rates in the sediment, a redundancy analysis (RDA) was performed on the nitrate reduction rates (NRR), nitrite production (NiPR) and ammonium production (APR) rates, with a stepwise selection of explanatory variables (Figure 4). The reaction rates determined using the flow-through reactors were explained at 83% by four selected parameters, which were the concentrations in both phaeopigments and in chlorophyll *a*, the HMW carbohydrate and the HMW protein fraction of the EPS (Figure 4). The first axis of the RDA was correlated with Phaeo (Regression Score RS=0.98), the HMW carbohydrate fraction (RS=0.82), the HMW protein fraction (RS=0.64) and the LMW carbohydrate of EPS (RS=0.59). Like the PCA, the first axis separates the freshwater mudflat (FM) on the right part of the plot, whatever the sampling date, from the other sites and dates (Figure 4). The second axis of the RDA was mainly correlated with the LMW carbohydrate of EPS (RS=-0.64), the HMW protein fraction (RS=0.34) and the HMW carbohydrate of EPS (RS=0.29). The second axis separates samples (except for FM) collected in September at the bottom part of the plot and samples collected in March (and June for IM) at the top. The nitrate reduction rate (NRR) is linked to Phaeo and the HMW carbohydrate of EPS on the RDA (Figure 4), which is confirmed by a correlation between NRR and Phaeo parameters (Spearman correlation, r_S=0.85, $p<0.001$). NRR is also linked to LMW protein fraction of the EPS, as Phaeo and LMW protein are strongly correlated (r_S=0.85; $p<0.001$). In accordance with correlations observed in the PCA, we also find a correlation between NRR and N content ($r=0.72$; $p<0.05$). Similarly, in the RDA, ammonium production rate (APR) is linked to both HMW and LMW carbohydrate of EPS and Phaeo. The intermediate nitrite production rate (NiPR, data not shown) is more associated with the HMW protein fraction of the EPS and the LMW carbohydrate of EPS (Figure 4), however these correlations are not significant (r_S=0.34 and r_S=0.42 respectively; $p>0.05$).

4. DISCUSSION

All sediments adjacent to the Seine River showed a high potential for nitrate reduction. The role of these sediments as a nitrogen sink is in line with the low nitrate concentrations at the sampling sites (0-200 µM NO_3^- except one high value of 400 µM NO_3^- at the RW) compared to concentrations in the Seine river water column (350-500 µM NO_3^-). In agreement with our hypothesis, nitrate reduction rates were not correlated to the total organic carbon (C_{org}) quantity of the sediments. A strong positive correlation was observed between nitrate reduction rates, phaeopigments and chlorophyll *a*, suggesting a role of freshly degraded algae in nitrate reduction. The presence of the algae also seems to affect ammonium production rates, strongly correlated to chl *a* and the carbohydrate and protein EPS fractions, via mineralization of the algal biomass. The more general indicators for carbon quality, biodegradable carbon fraction and C_{org}:N ratio, showed neither correlation with nitrate reduction nor ammonium production rates.

4.1 Biodegradable carbon

The degradable organic carbon content in these riparian, estuarine sediments ranged between 9 and 44 % of the total amount of organic carbon with a strong, significant correlation between total organic and degradable carbon (Spearman correlation, r_S = 0.685, p = 0.017). Similar fractions of biodegradable carbon were determined using the same approach in suspended matter, between 10 and 25%, in the water column of the Seine River (Servais and Garnier, 2006) and between 3 and 13 % in intact estuarine sediments under nitrate reducing conditions in the Scheldt River, Belgium (Abell et al., 2009). The lack of correlation between the amount of degradable carbon fraction and nitrate reduction rates suggests that this fraction is a poor indicator for nitrate reduction rates. The measured nitrate reduction rates in this study were determined on fresh sediment over a relative short period (48 h). The biodegradable carbon estimation (Servais et al., 1999) is also determined on fresh sediment, under optimal conditions (i.e. homogenized, aerobic) over a period of 40 days. It is generally considered that organic matter is made up of an infinite number of fractions with variable degradability, decreasing over time (Boudreau and Ruddick, 1991). This change over time in carbon degradability most likely explains the lack of correlation between nitrate reduction rates

433 determined over a short period, degrading the most labile carbon fraction, and the amount of
434 carbon degraded over a longer time period including a larger range of carbon degradability.
435
436
437
438 ***4.2 Nitrate reduction rates related to sediment organic carbon: the role of microalgae.***

439 A strong correlation between the amount of phaeopigments as well as chl*a* and nitrate
440 reduction rates suggests an important role of the presence of microalgae. This correlation might
441 indicate microalgal activity regarding nitrate reduction or consumption; nitrate assimilation by
442 microphytobenthos (MPB) has been shown to occur and even exceeds denitrification in
443 estuarine sediments (Sundback and Miles, 2000). This phenomenon is mainly related to low
444 nitrate availability and photosynthetic conditions. Nitrate can also be stored by diatoms (Kamp
445 et al., 2011), in vacuoles and used under anoxic conditions. Both assimilation and storage of
446 nitrate seems unlikely as nitrate reduction rates were determined at high nitrate concentrations
447 in the dark. The strong correlation of nitrate reduction with phaeopigments, the degraded form
448 of chl *a*, suggests rather the use of dead or senescing algal biomass as a carbon source for nitrate
449 reduction. This was also shown by a strong increase in nitrate reduction rates upon the addition
450 of dried algal material (data not shown). This is in agreement with previous studies, showing a
451 stimulation of denitrification rates by the addition of senescing algal biomass providing N and
452 labile C to denitrifiers in agricultural headwater stream sediments (McMillan et al., 2010). A
453 positive correlation was also demonstrated in wetland and pond sediments between
454 denitrification rates and the presence of diatoms (Ishida et al., 2008). The positive correlation
455 between nitrate reduction rates and certain fractions of the EPS secreted by MPB indicates a
456 more indirect effect of the algal presence on nitrate reduction. Nitrate reduction benefits in this
457 case from EPS that was produced by algae. Exudates of different algal species stimulated
458 denitrification rates and influenced the denitrifying community structure of periphytic biofilms
459 (Kalscheur et al., 2012; McMillan et al., 2010). A similar positive effect of EPS, *via* the addition
460 of MPB biomass, on denitrifier abundance, determined *via* qPCR of *nirS* and *nirK* genes, was
461 observed in intertidal sediments (Decleyre et al., 2015). It appears that the positive correlation
462 between the presence of algal biomass and nitrate reduction rates is due to the supply of organic
463 carbon, either excreted as EPS or the use of algal biomass as a labile carbon source. The addition
464 of dried algal biomass as carbon source confirms this phenomenon (data not shown).

Denitrification can be stimulated by using the extracellular carbon secreted by algae (Wotton 2004) in addition to organic carbon from dead organisms.

Despite representing a relative small fraction of the total organic carbon content, the algal biomass and the EPS carbohydrates are strongly correlated to nitrate reduction rates. A comparison of the different carbon fractions determined in this study is shown in Table 3. The amount of algal biomass in carbon units was deduced from the amount of chlorophyll *a* using a factor of 35 µgC algal biomass per µg chl*a* (Garnier et al., 1989), the EPS HMW and LMW carbohydrates were converted considering the glucose equivalents used in the analysis (Dubois et al., 1956). The protein fraction, less than 3 % of the EPS fraction, was not considered. The algal biomass, based on the chlorophyll *a* quantities present in the sediment, made up 0.5 to 5.2% of the total organic carbon fraction. Considering this fraction being biodegradable the algal biomass would contribute between 2 and 20.5% to the biodegradable carbon in the different sediments. The algal fraction of total organic carbon as well as the degradable fraction was lowest (0.5 and 2% respectively) in the riverine wetland sediment, whereas the presence and contribution to the carbon pools was high at the other sites (3.3-5.2% and 15.1-20.5%). This is in good agreement with the C_{org}:N ratio (less than 11) of the organic matter indicating that the origin of organic matter is mainly algal at the AW, FM et IM, whereas the high C_{org}:N ratios at the RW indicates a terrestrial origin (Meyers, 1994).

The EPS fraction made up less than 1.5 % of the total organic carbon pool and between 1.8 and 6.3% of the degradable carbon in these sediments. Despite the small variation in total carbohydrates EPS contents, the contribution of this fraction to the BDOC showed differences between the sediments; the highest fraction of carbohydrate EPS relative to the amount of BDOC was found in the artificial wetland sediment, with an average of 6.3%. with lower proportions in the other sediments (1.8-3.3%).

4.3 Impact of microalgae and their exopolysaccharides secretions on nitrate reduction

The strong correlations between phaeopigments and nitrate reduction rates as well as between the N content and low molecular weight (LMW) proteins as well as high molecular weight (HMW) carbohydrates suggest a potential role for the EPS fraction as a source of organic matter in nitrate reduction rates. The LMW compounds are likely the most labile form of EPS (Welker et al., 2002), which is in good agreement with the positive correlation between the LMW protein and nitrate reduction rates. The HMW carbohydrates are degraded by

498 exoenzymatic activity into labile LMW compounds (Van Duyl et al 1999), subsequently
499 available for nitrate reduction.

500 The low molecular weight EPS fraction is continuously secreted by living microalgae
501 (Orvain et al., 2014) while secretion of high molecular weight EPS is rather controlled by
502 environmental conditions like irradiance, temperature or salinity (Underwood et al., 2004)
503 rather to protect cells from dehydration or osmotic shock. The seasonal and spatial presence of
504 microalgae and the excretion of the different EPS fractions may thus have implications on
505 nitrate reduction rates in intertidal sediments.

506 Overall, the EPS concentrations showed little seasonal but rather site variation. The protein
507 fraction was generally low and never exceeded 3% of the carbohydrate fraction, which is in
508 good agreement with previous observations in intertidal mudflats (Orvain et al., 2014). High
509 chlorophyll *a* contents in March and/or September in the different sediments are in good
510 agreement with typical peaks of microalgae biomass in spring and autumn (Kwon et al., 2016).
511 In general the correlations between the different EPS fractions (LMW and HMW proteins,
512 HMW carbohydrates) and phaeopigment concentrations and to a lesser extent chlorophyll *a*
513 link the presence of EPS to the degradation status of the pigments, particularly in summer. The
514 relative high phaeopigments concentrations, exceeding the chlorophyll *a* contents, reveal the
515 presence of death algal biomass, being degraded, rather than active production of EPS by the
516 microalgae in these sediments. The high phaeopigment content, the degradation product of chl*a*,
517 in summer suggests senescing MPB. This could enhance release of internal EPS into the
518 environment during MPB cell lysis and/or grazing by benthic fauna (Hubas et al., 2010; van
519 der Wal et al., 2010), thus becoming available for microbial nitrate reduction during this period.

520 The higher contribution of carbohydrates and proteins in the BDOC in the intertidal
521 mudflat (5.9-15.6% of BDOC) than in the freshwater mudflat (3.8-9.6% of BDOC) could be
522 due to a higher secretion of EPS in the intertidal mudflat than in the freshwater mudflat. It has
523 been shown that EPS secretion protects benthic microalgae against salinity, and prevents drying
524 of algal cells at low tide (Orvain et al., 2014). The difference in contribution of carbohydrates
525 and proteins in the BDOC between the riparian wetland (2.9-6.9%) and the artificial wetland
526 (11.7-41.9%) seems rather due to the higher import of BDOC in the riparian wetland than in
527 the artificial one. Indeed, the riparian wetland located near the dam of Poses in the upper part
528 of the estuary, receives relative high DOC quantities from the river (on average 4 ± 2.3 mg
529 DOC L^{-1}) which decrease during the water residence time in the freshwater estuary with a
530 recycling of organic matter estimated between 40 and 70% (Garnier et al., 2008).

The different EPS fractions were related to the measured nitrogen cycling rates. These associations confirm the potential role of microalgae, *via* their secretions (EPS) in the microbial degradation and nitrate reduction. Based on these observations and on the results of this study, the artificial wetland seems to be the location where algae and EPS were the most important as a support to bacterial denitrification especially in spring (March).

Conclusions

In the investigated sediments, nitrate reduction rates were neither explained by total organic carbon contents nor the biodegradable carbon fraction. Interestingly a strong positive correlation between the algal biomass and nitrate reduction indicates a role for microalgae in benthic nitrate elimination. We hypothesize that the presence of EPS, excreted by microalgae is the main supplier of organic carbon fueling nitrate reduction. This is in line with the degradation and incorporation of EPS by heterotrophic bacteria in intertidal sediments (Bellinger et al., 2009; Taylor et al., 2013). The presence of microalgae at the surface of intertidal mudflat sediments plays an important role stimulating nitrate reduction and thus the mitigation of excess nitrate. The excess nitrate has led to coastal eutrophication, with the occurrence of harmful algal blooms in the Seine Bay (Thorel et al., 2017). In the agricultural dominated Seine Basin N fluxes remain stable with little perspective of significant decrease, (Garnier et al., 2019). Our results confirm the role of intertidal mudflats and the presence of microalgae in biogeochemical nitrogen cycling. Conservation of intertidal mudflats, regarding the role as nitrogen sink, seems thus important. In the Seine Estuary, undergoing a strong decrease in the surface of intertidal mudflats (Lesourd et al., 2016), restauration of these areas might be favorable mitigating nitrogen pollution.

Sample CRediT author statement

Anniet Laverman: Conceptualization, Methodology, Investigation, Writing- Original draft preparation, Writing- Reviewing and Editing, Funding acquisition. **Céline Roose-Amsaleg:** Investigation, Writing- Reviewing and Editing**. Jerome Morelle**: Investigation, Writing- Reviewing and Editing. **Alexandrine Pannard:** Formal analysis, Writing- Reviewing and Editing.

563

564 ***ACKNOWLEDGEMENTS***

565 The authors thank Olivier Tronquart, Benjamin Mercier, Simon Decock for nutrient,
566 BDOC, chlorophyll analysis and assistance in the field; Aurelien Baro for his help with figure
567 1 and Henri Etcheber for total carbon and nitrogen analysis (EPOC, Bordeaux). This study was
568 financed by the RE2 Project (SAIV2009-RE2-1) in the GIP Seine-Aval 4 program. Two
569 anonymous reviewers are acknowledged for their valuable comments on our manuscript.

570 ***References***

571

572 Abell, J., Laverman, A.M. and Van Cappellen, P. 2009. Bioavailability of organic matter
573 in a freshwater estuarine sediment: long-term degradation experiments with and without
574 nitrate supply. Biogeochemistry 94(1), 13-28.
575 Arango, C.P., Tank, J.L., Schaller, J.L., Royer, T.V., Bernot, M.J. and David, M.B. 2007.
576 Benthic organic carbon influences denitrification in streams with high nitrate
577 concentration. Freshwater Biology 52(7), 1210-1222.
578 Bastviken, S.K., Eriksson, P.G., Ekstrom, A. and Tonderski, K. 2007. Seasonal
579 denitrification potential in wetland sediments with organic matter from different plant
580 species. Water Air and Soil Pollution 183(1-4), 25-35.
581 Bellinger, B.J., Underwood, G.J.C., Ziegler, S.E. and Gretz, M.R. 2009. Significance of
582 diatom-derived polymers in carbon flow dynamics within estuarine biofilms determined
583 through isotopic enrichment. Aquatic Microbial Ecology 55(2), 169-187.
584 Blanchet, F.G., Legendre, P. and Borcard, D. 2008. Forward selection of explanatory
585 variables. Ecology 89(9), 2623-2632.
586 Bohorquez, J., McGenity, T.J., Papaspyrou, S., Garcia-Robledo, E., Corzo, A. and
587 Underwood, G.J.C. 2017. Different Types of Diatom-Derived Extracellular Polymeric
588 Substances Drive Changes in Heterotrophic Bacterial Communities from Intertidal
589 Sediments. Frontiers in Microbiology 8, 16.
590 Borcard, D., Gillet, F. and Pierre, L. (2011) Numerical ecology with R.
591 Boudreau, B.P. and Ruddick, B.R. 1991. On A Reactive Continuum Representation Of
592 Organic-Matter Diagenesis. American Journal Of Science 291(5), 507-538.
593 Burford, J.R. and Bremner, J.M. 1975. Relationships between the denitrification
594 capacities of soils and total, water-soluble and readily decomposable soil organic matter.
595 7(6), 389.
596 Cugier, P., Billen, G., Guillaud, J.F., Garnier, J. and Menesguen, A. 2005. Modelling
597 the eutrophication of the Seine Bight (France) under historical, present and future
598 riverine nutrient loading. Journal Of Hydrology 304(1-4), 381-396.
599 Decleyre, H., Heylen, K., Sabbe, K., Tytgat, B., Deforce, D., Van Nieuwerburgh, F., Van
600 Colen, C. and Willems, A. 2015. A Doubling of Microphytobenthos Biomass
601 Coincides with a Tenfold Increase in Denitrifier and Total Bacterial Abundances in
602 Intertidal Sediments of a Temperate Estuary. Plos One 10(5).
603 Dodla, S.K., Wang, J.J., DeLaune, R.D. and Cook, R.L. 2008. Denitrification potential
604 and its relation to organic carbon quality in three coastal wetland soils. Science of the
605 Total Environment 407(1), 471-480.
606 Dubois, M., Gilles, K.A., Hamilton, J.K., Rebers, P.A. and Smith, F. 1956. Colorimetric
607 method for the determination of sugars and related substances. Analytical Chemistry
608 28(3), 350-356.
609 Fernandes, S.O., Dutta, P., Gonsalves, M.-J., Bonin, P.C. and LokaBharathi, P.A. 2016.
610 Denitrification activity in mangrove sediments varies with associated vegetation.
611 Ecological Engineering 95, 671-681.
612 Galloway, J.N., Dentener, F.J., Capone, D.G., Boyer, E.W., Howarth, R.W., Seitzinger,
613 S.P., Asner, G.P., Cleveland, C.C., Green, P.A., Holland, E.A., Karl, D.M., Michaels,
614 A.F., Porter, J.H., Townsend, A.R. and Vorosmarty, C.J. 2004. Nitrogen cycles: past,
615 present, and future. Biogeochemistry 70(2), 153-226.

Garnier, J., Billen, G., Even, S., Etcheber, H. and Servais, P. 2008. Organic matter dynamics and budgets in the turbidity maximum zone of the Seine Estuary (France). Estuarine Coastal and Shelf Science 77(1), 150-162.

Garnier, J., Blanc, P. and Benest, D. 1989. Estimating a carbon chlorophyll ratio in nanoplankton (Creteil Lake, S-E Paris, France). Water Resources Bulletin 25(4), 751-754.

Garnier, J., Riou, P., Le Gendre, R., Ramarson, A., Billen, G., Cugier, P., Schapira, M., Thery, S., Thieu, V. and Menesguen, A. 2019. Managing the Agri-Food System of Watersheds to Combat Coastal Eutrophication: A Land-to-Sea Modelling Approach to the French Coastal English Channel. Geosciences 9(10).

Griffiths, R.I., Whiteley, A.S., O'Donnell, A.G. and Bailey, M.J. 2000. Rapid method for coextraction of DNA and RNA from natural environments for analysis of ribosomal DNA- and rRNA-based microbial community composition. Applied and Environmental Microbiology 66(12), 5488-5491.

Groffman, P.M., Axelrod, E.A., Lemunyon, J.L. and Sullivan, W.M. 1991. Denitrification in grass and forest vegetated filter strips. Journal of Environmental Quality 20(3), 671-674.

Gu, C., Laverman, A.M. and Pallud, C.E. 2012. Environmental controls on nitrogen and sulfur cycles in surficial aquatic sediments. Frontiers in Microbiology 3.

Hill, A.R. and Cardaci, M. 2004. Denitrification and organic carbon availability in riparian wetland soils and subsurface sediments. Soil Science Society of America Journal 68(1), 320-325.

Howarth, R.W., Billen, G., Swaney, D., Townsend, A., Jaworski, N., Lajtha, K., Downing, J.A., Elmgren, R., Caraco, N., Jordan, T., Berendse, F., Freney, J., Kudeyarov, V., Murdoch, P. and Zhu, Z.L. 1996. Regional nitrogen budgets and riverine N&P fluxes for the drainages to the North Atlantic Ocean: Natural and human influences. Biogeochemistry 35(1), 75-139.

Howarth, R.W. and Marino, R. 2006. Nitrogen as the limiting nutrient for eutrophication in coastal marine ecosystems: Evolving views over three decades. Limnology And Oceanography 51(1), 364-376.

Hubas, C., Sachidhanandam, C., Rybarczyk, H., Lubarsky, H.V., Rigaux, A., Moens, T. and Paterson, D.M. 2010. Bacterivorous nematodes stimulate microbial growth and exopolymer production in marine sediment microcosms. Marine Ecology Progress Series 419, 85-94.

Humbert, S., Zopfi, J. and Tarnawski, S.-E. 2012. Abundance of anammox bacteria in different wetland soils. Environmental Microbiology Reports 4(5).

Ishida, C.K., Arnon, S., Peterson, C.G., Kelly, J.J. and Gray, K.A. 2008. Influence of algal community structure on denitrification rates in periphyton cultivated on artificial substrata. Microbial Ecology 56(1), 140-152.

Kalscheur, K.N., Rojas, M., Peterson, C.G., Kelly, J.J. and Gray, K.A. 2012. Algal Exudates and Stream Organic Matter Influence the Structure and Function of Denitrifying Bacterial Communities. Microbial Ecology 64(4), 881-892.

Kamp, A., de Beer, D., Nitsch, J.L., Lavik, G. and Stief, P. 2011. Diatoms respire nitrate to survive dark and anoxic conditions. Proceedings of the National Academy of Sciences of the United States of America 108(14), 5649-5654.

Kassambara, A. and Mundt, F. 2017 "Package 'factoextra'." Extract and visualize the results of multivariate data analyses.

Kloos, K., Mergel, A., Rosch, C. and Bothe, H. 2001. Denitrification within the genus Azospirillum and other associative bacteria. Australian Journal Of Plant Physiology 28(9), 991-998.

Knowles, R. 1982. Denitrification. Microbial Reviews 46(1), 43-70.
Kwon, B.-O., Lee, Y., Park, J., Ryu, J., Hong, S., Son, S., Lee, S.Y., Nam, J., Koh, C.-H. and Khim, J.S. 2016. Temporal dynamics and spatial heterogeneity of microalgal biomass in recently reclaimed intertidal flats of the Saemangeum area, Korea. Journal of Sea Research 116, 1-11.
Laverman, A.M., Van Cappellen, P., van Rotterdam-Los, D., Pallud, C. and Abell, J. 2006. Potential rates and pathways of microbial nitrate reduction in coastal sediments. FEMS Microbiology Ecology 58(2), 179-192.
Lesourd, S., Lesueur, P., Fisson, C. and Dauvin, J.-C. 2016. Sediment evolution in the mouth of the Seine estuary (France): A long-term monitoring during the last 150 years. Comptes Rendus Geoscience 348(6), 442-450.
Lorenzen, C.J. 1967. Determination of chlorophyll and pheo-pigments - spectrophotometric equations. Limnology and Oceanography 12(2), 343-&.
Marchesi, J.R., Sato, T., Weightman, A.J., Martin, T.A., Fry, J.C., Hiom, S.J. and Wade, W.G. 1998. Design and evaluation of useful bacterium-specific PCR primers that amplify genes coding for bacterial 16S rRNA. Appl Environ Microbiol 64(2), 795-799.
McMillan, S.K., Piehler, M.F., Thompson, S.P. and Paerl, H.W. 2010. Denitrification of Nitrogen Released from Senescing Algal Biomass in Coastal Agricultural Headwater Streams. Journal of Environmental Quality 39(1), 274-281.
Meyers, P.A. 1994. Preservation of elemental and isotopic source identification of sedimentary organic-matter. Chemical Geology 114(3-4), 289-302.
Mohan, S.B., Schmid, M., Jetten, M. and Cole, J. 2004. Detection and widespread distribution of the nrfA gene encoding nitrite reduction to ammonia, a short circuit in the biological nitrogen cycle that competes with denitrification. Fems Microbiology Ecology 49(3), 433-443.
Muyzer, G., de Waal, E.C. and Uitterlinden, A.G. 1993. Profiling of complex microbial populations by denaturing gradient gel electrophoresis analysis of polymerase chain reaction-amplified genes coding for 16S rRNA. Applied and Environmental Microbiology 59(3), 695-700.
Orvain, F., De Crignis, M., Guizien, K., Lefebvre, S., Mallet, C., Takahashi, E. and Dupuy, C. 2014. Tidal and seasonal effects on the short-term temporal patterns of bacteria, microphytobenthos and exopolymers in natural intertidal biofilms (Brouage, France). Journal of Sea Research 92, 6-18.
Pallud, C., Meile, C., Laverman, A.M., Abell, J. and Van Cappellen, P. 2007. The use of flow-through sediment reactors in biogeochemical kinetics: Methodology and examples of applications. Marine Chemistry 106(1-2), 256-271.
Pallud, C. and Van Cappellen, P. 2006. Kinetics of microbial sulfate reduction in estuarine sediments. Geochimica Et Cosmochimica Acta 70, 1148-1162.
Passow, U. 2002. Transparent exopolymer particles (TEP) in aquatic environments. Progress in Oceanography 55(3-4), 287-333.
Pignolet, O., Jubeau, S., Vaca-Garcia, C. and Michaud, P. 2013. Highly valuable microalgae: biochemical and topological aspects. Journal of Industrial Microbiology & Biotechnology 40(8), 781-796.
Roychoudhury, A., Viollier, E. and Van Cappellen, P. 1998. A plug flow-through reactor for studying biogeochemical reactions in undisturbed aquatic sediments. Applied Geochemistry 13, 269-280.
Schipper, L.A., Harfoot, C.G., McFarlane, P.N. and Cooper, A.B. 1994. Anaerobic decomposition and dentrification during plant decomposition in an organic soil. Journal of Environmental Quality 23(5), 923-928.

Servais, P. and Garnier, J. 2006. Organic carbon and bacterial heterotrophic activity in the maximum turbidity zone of the Seine estuary (France). Aquatic Sciences 68(1), 78-85.

Servais, P., Garnier, J., Demarteau, N., Brion, N. and Billen, G. 1999. Supply of organic matter and bacteria to aquatic ecosystems through waste water effluents. Water Research 33(16), 3521-3531.

Sirivedhin, T. and Gray, K.A. 2006. Factors affecting denitrification rates in experimental wetlands: Field and laboratory studies. Ecological Engineering 26(2), 167-181.

Strous, M., Fuerst, J.A., Kramer, E.H.M., Logemann, S., Muyzer, G., van de Pas-Schoonen, K.T., Webb, R., Kuenen, J.G. and Jetten, M.S.M. 1999. Missing lithotroph identified as new planctomycete. Nature 400(6743), 446-449.

Sundback, K. and Miles, A. 2000. Balance between denitrification and microalgal incorporation of nitrogen in microtidal sediments, NE Kattegat. Aquatic Microbial Ecology 22(3), 291-300.

Taylor, J.D., McKew, B.A., Kuhl, A., McGenity, T.J. and Underwood, G.J.C. 2013. Microphytobenthic extracellular polymeric substances (EPS) in intertidal sediments fuel both generalist and specialist EPS-degrading bacteria. Limnology and Oceanography 58(4), 1463-1480.

Thorel, M., Claquin, P., Schapira, M., Le Gendre, R., Riou, P., Goux, D., Le Roy, B., Raimbault, V., Deton-Cabanillas, A.-F., Bazin, P., Kientz-Bouchart, V. and Fauchot, J. 2017. Nutrient ratios influence variability in Pseudo-nitzschia species diversity and particulate domoic acid production in the Bay of Seine (France). Harmful Algae 68, 192-205.

Thouvenot, M., Billen, G. and Garnier, J. 2007. Modelling nutrient exchange at the sediment-water interface of river systems. Journal of Hydrology 341(1-2), 55-78.

Tiedje, J.M. 1988. Ecology of denitrification and dissimilatory nitrate reduction to ammonium.

Tiedje, J.M., Sextone, A.J., Myrold, D.D. and Robinson, J.A. 1982. Denitrification: Ecological niches, competition and survival. Antonie Van Leeuwenhoek 48, 569-583.

Underwood, G.J.C., Boulcott, M., Raines, C.A. and Waldron, K. 2004. Environmental effects on exopolymer production by marine benthic diatoms: Dynamics, changes in composition, and pathways of production. Journal of Phycology 40(2), 293-304.

Underwood, G.J.C. and Paterson, D.M. (2003) Advances in Botanical Research, Vol 40. Callow, J.A. (ed), pp. 183-240.

van der Wal, D., Wielemaker-van den Dool, A. and Herman, P.M.J. 2010. Spatial Synchrony in Intertidal Benthic Algal Biomass in Temperate Coastal and Estuarine Ecosystems. Ecosystems 13(2), 338-351.

Vandegraaf, A.A., Mulder, A., Debruijn, P., Jetten, M.S.M., Robertson, L.A. and Kuenen, J.G. 1995. Anaerobic Oxidation Of Ammonium Is A Biologically Mediated Process. Applied And Environmental Microbiology 61(4), 1246-1251.

Welsh, A., Chee-Sanford, J.C., Connor, L.M., Loeffler, F.E. and Sanford, R.A. 2014. Refined NrfA Phylogeny Improves PCR-Based nrfA Gene Detection. Applied and Environmental Microbiology 80(7), 2110-2119.

Welker, C., Sdrigotti, E., Covelli, S. and Faganeli, J. 2002. Microphytobenthos in the Gulf of Trieste (Northern Adriatic Sea): Relationship with labile sedimentary organic matter and nutrients. Estuarine Coastal and Shelf Science 55(2), 259-273.

764 TABLES AND FIGURES

765

766 **Table 1. Bacterial abundance (*16S rRNA* gene), denitrifying (*nosZ* gene), DNRA (*nrfA* gene) and anammox**
767 **(amx *16S rRNA* gene, "amx") as well as the percentages of the different functional groups of the total bacterial**
768 **abundance expressed as gene copie vs 16S determined *via* qPCR.**

769

Site		LOG 16s (copie gds^{-1})	LOG nosZ	LOG nrfA	LOG amx	nosZ :16s %	Nrf :16s	Amx :16s
RW	March	9.6	8.3	7.2	5.7	4.9	0.4	0.01
	June	9.2	8.0	6.9	5.2	7.2	0.5	0.01
	Sept	9.3	7.9	6.9	5.4	4.4	0.4	0.01
AW	March	9.2	7.5	6.5	b.d.	2.3	0.2	-
	June	9.4	7.7	7.0	b.d.	2.2	0.4	-
	Sept	9.7	8.1	6.8	b.d.	2.6	0.1	-
FM	March	10.1	8.7	7.2	6.1	4.2	0.1	0.01
	June	9.5	8.3	7.4	b.d.	5.6	0.8	-
	Sept	9.5	8.4	7.5	b.d.	6.9	0.8	-
IM	March	9.5	8.1	7.1	5.3	3.6	0.4	0.01
	June	9.3	7.8	6.7	b.d.	3.4	0.3	-
	Sept	9.4	7.9	6.8	b.d.	3.0	0.2	-

770 b.d.: below detection limit

Table 2. Characteristics of the sediment at the sampling sites (see figure 1) at the time of sampling. The sediment characteristics include organic carbon (C_{org}) and nitrogen (N) content, C_{org}: N ratio, biodegradable carbon (BDOC), chlorophyll *a* (chl *a*), phaeopigments (phaeo), EPS carbohydrates HMW and LMW (carb HMW, carb LMW), EPS proteins (prot HMW and LMW) concentrations.

775

Site	Season	C_{org}	N	C_{org} :N	BDOC	*BDOC: C_{org}*	chl *a*	phaeo	EPS			
									carb HMW	carb LMW	prot HMW	prot LMW
		%		mol :mol	mg gds^{-1}	%	ug gds^{-1}					
RW	March	5.67	0.15	44.1	13.6	*24*	3.3	13.2	185.3	203.7	0.31	0.69
	June	2.51	0.45	6.5	6.1	*24*	8.5	47.9	227.7	189.2	0.19	2.33
	Sept	3.68	0.14	30.7	5.8	*16*	7.5	15.7	187.6	174.2	1.69	1.30
AW	March	1.18	0.24	5.9	1.0	*9*	6.3	5.3	237.8	177.7	2.58	1.15
	June	1.68	0.36	5.4	3.2	*19*	5.6	80.3	194.3	187.8	3.27	2.04
	Sept	1.38	0.16	10.4	3.3	*24*	31.9	42.7	193.9	189.1	2.49	b.d.
FM	March	4.43	0.50	10.4	11.9	*27*	123.5	253.0	275.0	186.2	4.49	4.22
	June	5.56	0.98	6.7	13.8	*25*	20.7	611.3	312.6	201.6	5.47	6.99
	Sept	5.63	0.73	9.0	5.7	*10*	104.7	392.9	246.2	293.4	5.78	4.41
IM	March	1.56	0.18	10.4	6.8	*44*	7.4	31.5	188.8	205.3	2.58	2.36
	June	2.80	0.45	7.3	4.9	*18*	15.4	72.8	198.8	190.3	8.45	2.98
	Sept	2.25	0.28	9.5	2.4	*11*	62.8	63.6	174.2	191.6	2.01	2.79

780

Table 3. The different carbon fractions in the sediments expressed in units C averaged per site. HMW and LMW carbohydrates were converted based on the glucose standard and chlorophyll *a* contents were converted with a factor 35 according to Garnier et al (1989).

site	C_{org}	BDOC	algal biomass	EPS	algal biomass: C_{org}	algal biomass: BDOC	EPS: C_{org}	EPS:BDOC
		mgC gds^{-1}				**%**		
RW	31.05	8.48	0.17	0.16	0.5%	2.0%	0.5%	1.8%
AW	11.62	2.51	0.38	0.16	3.3%	15.1%	1.4%	6.3%
FM	41.59	10.48	2.15	0.20	5.2%	20.5%	0.5%	1.9%
IM	17.34	4.70	0.74	0.15	4.3%	15.7%	0.9%	3.3%

785

790

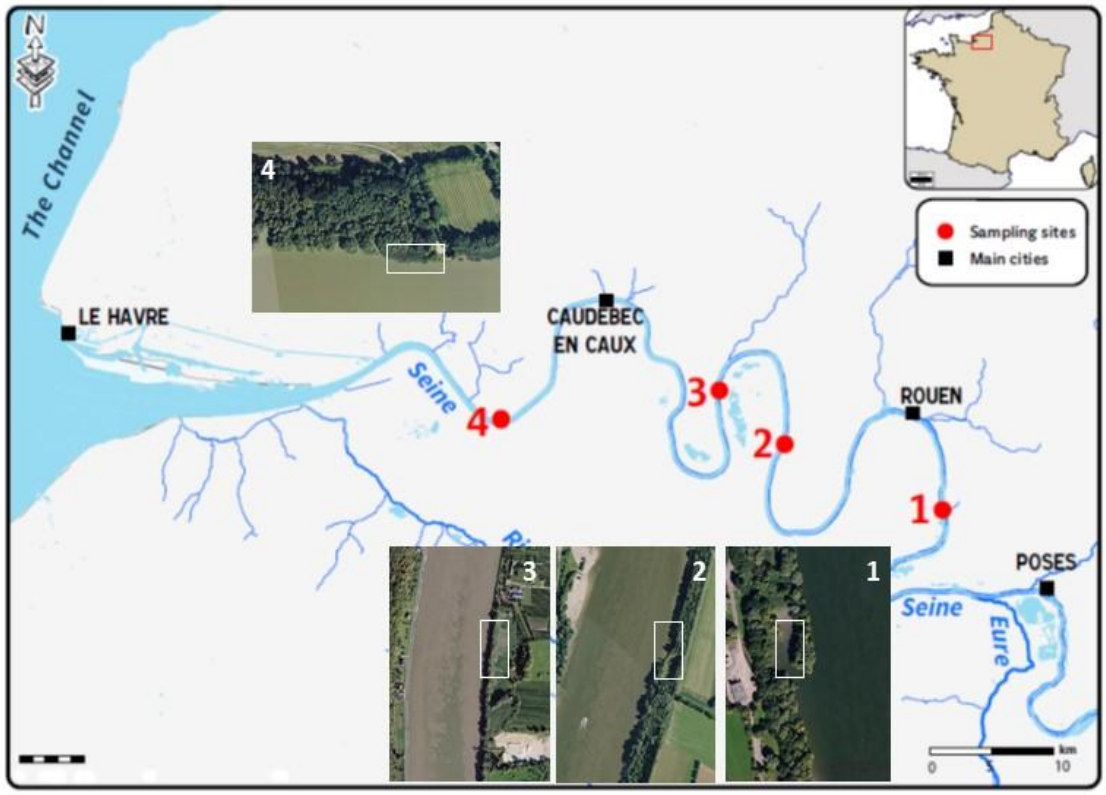

Figure 1. sampling sites from upstream to downstream: (1) riparian wetland RW, (2) artificial wetland AW (3) freshwater mudflat FW and (4) intertidal mudflat IM. The rectangles indicate the 795 **locations of the sampling sites. A weir at Poses (upstream of site 1) limits the tidal influence, whereas the upstream limit of saline intrusion is at Caudebex en Caux.**

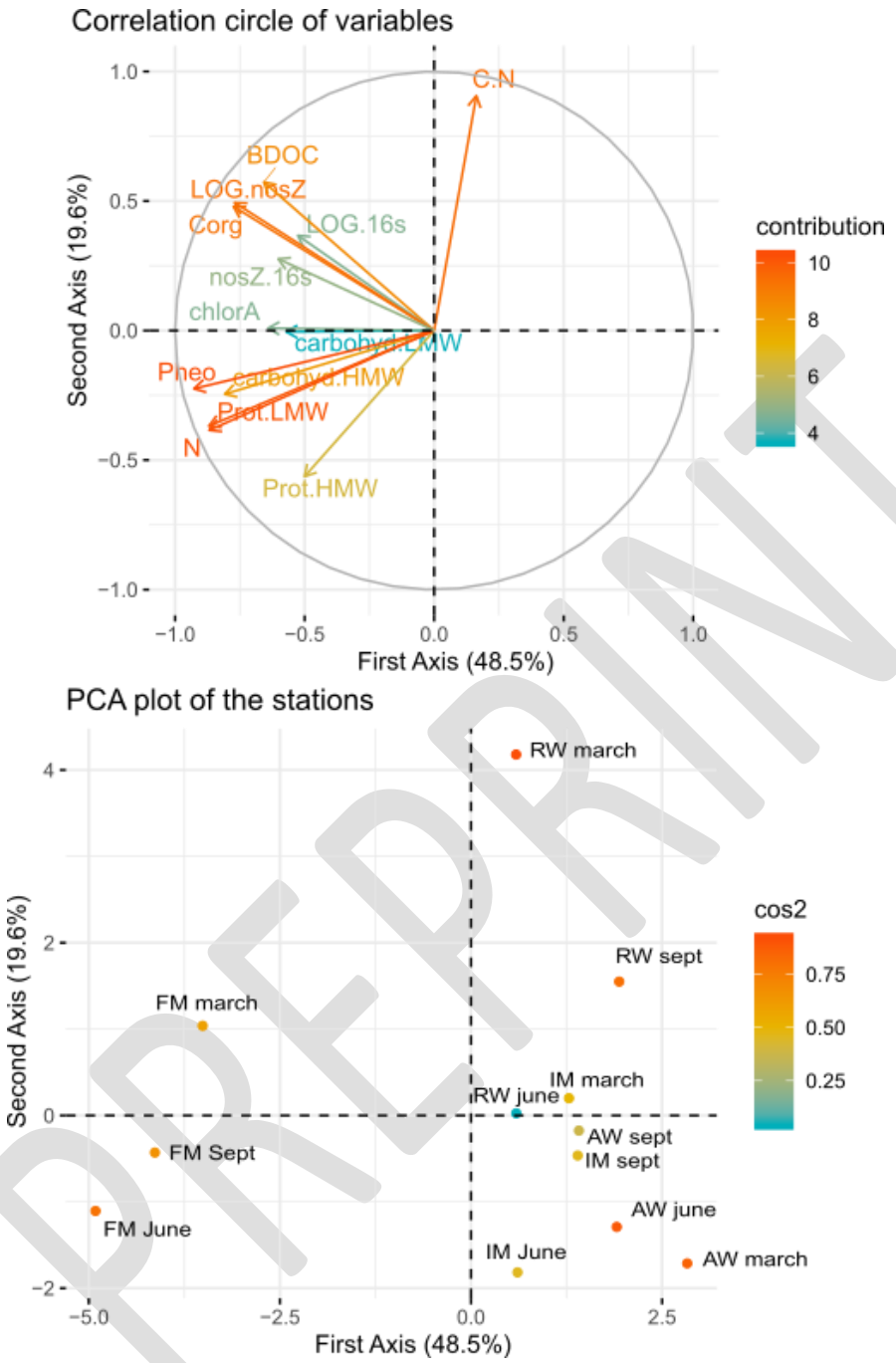

Figure 2. First two principal axes of the Principal component analysis performed on the sediment characteristics from the sample stations, riverine wetland (RW), artificial wetland (AW), freshwater mudflat (FM) and intertidal mudflat (IM), during the 3 different sampling dates (March, June and September), see section 2.2 for details. Upper right: site scores colored by contribution to axes. Bottom: factor scores of the variables colored by contribution to axes. The square cosine (square of the correlation coefficient with PCA axis) gives the quality of the representation of each variable on PCA axis.

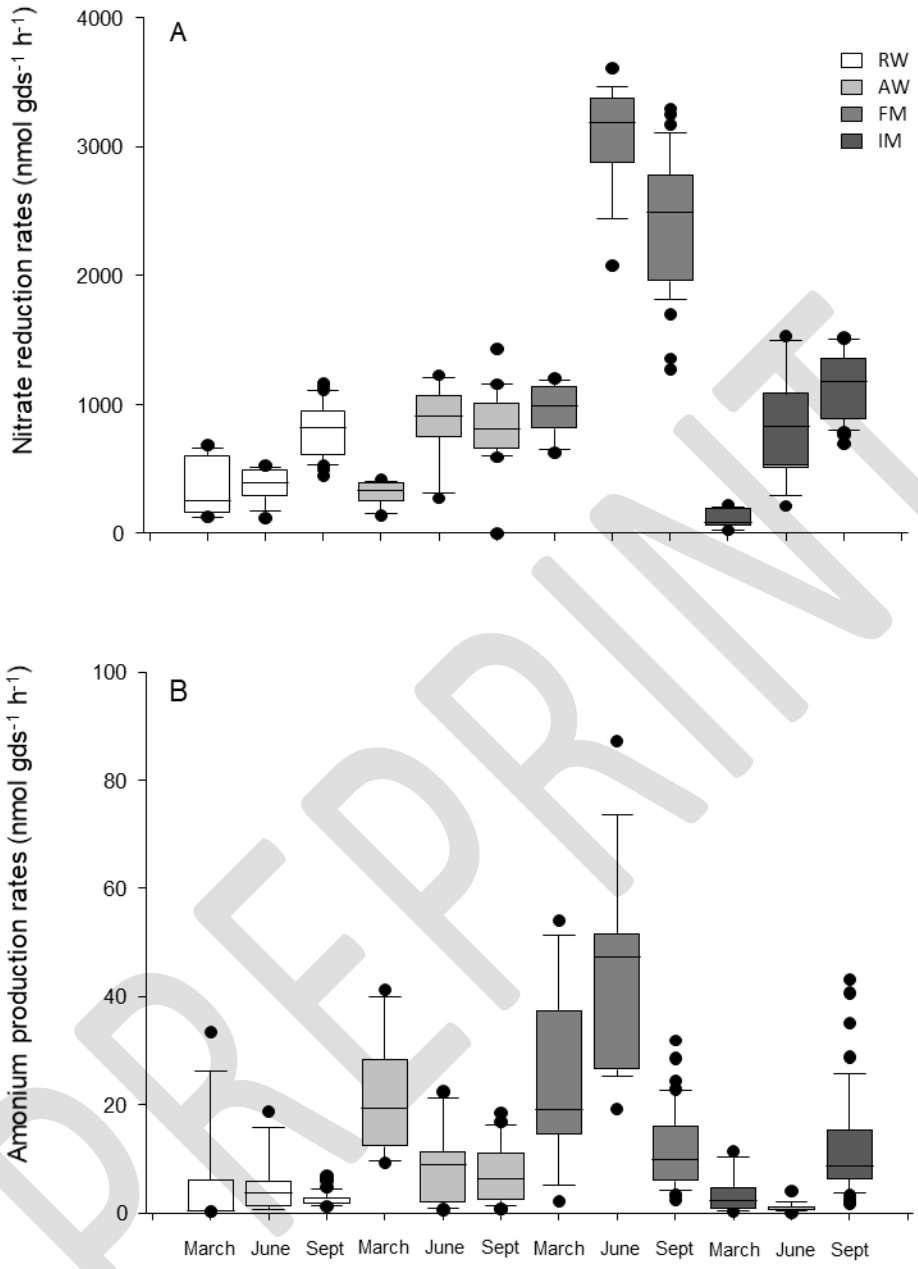

Figure 3. Box plots of the nitrate reduction and ammonium production rates at the 4 sites riverine wetland (RW), artificial wetland (AW), freshwater mudflat (FM) and intertidal mudflat (IM) along the Seine River at the 3 different sampling dates, March (n=12), June (n=12)and September (n=36, except FM n=26), see section 2.2 for details. Boxes encompass the upper and lower quartiles while the line indicates the median, dots are outliers.

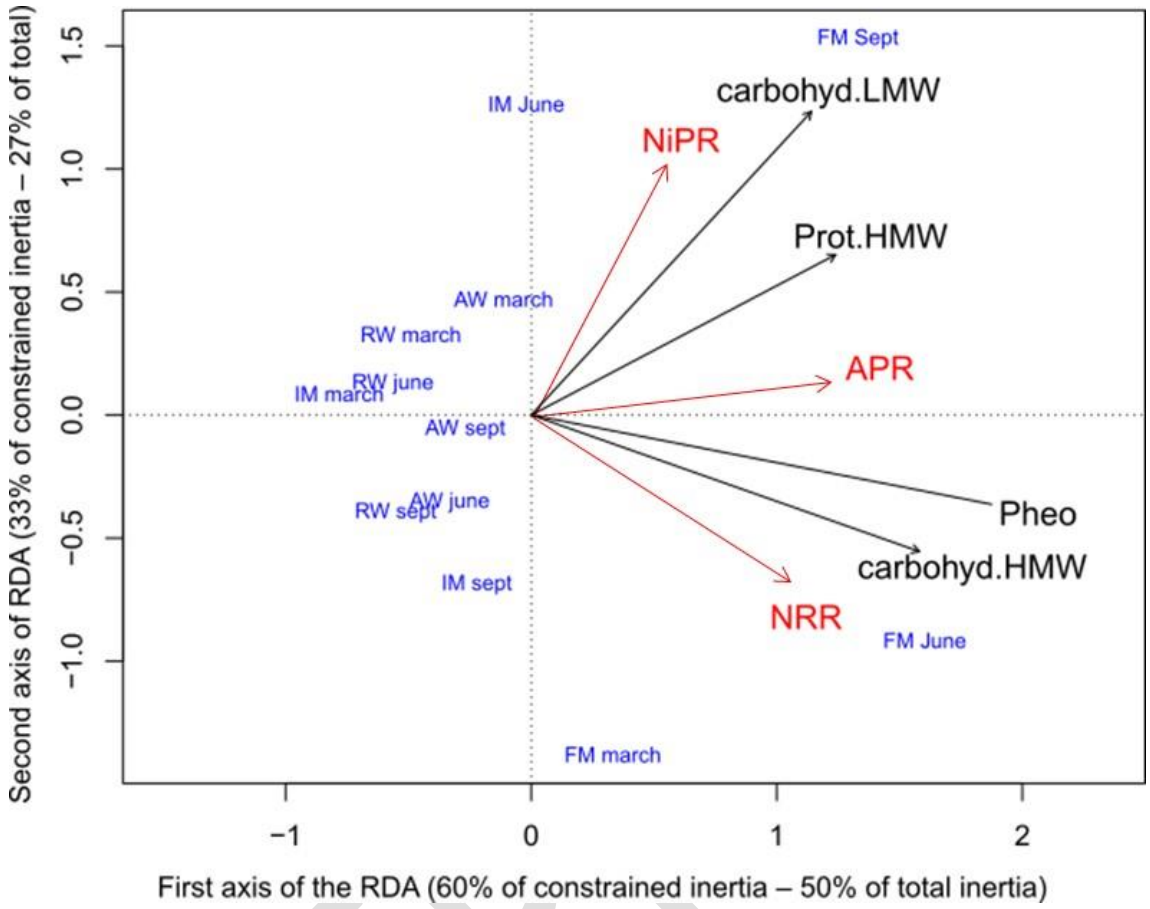

Figure 4. Ordination triplots of the first two axes of the Redundancy Analysis (RDA) between the reaction rates (NRR, NiPR and APR) and the chemical characteristics of the sediment after forward selection (78.9% of constrained variance – 21.1% of residuals). The plot corresponds to the scaling 2, which preserves correlations between descriptors. The reaction rates measured at the different sites, riverine wetland (RW), artificial wetland (AW), freshwater mudflat (FM) and intertidal mudflat (IM), and sampling dates (red vectors) are explained by four chemical parameters selected by the model (blue vectors). Vectors pointing in the same direction indicate a positive correlation, while vectors pointing in opposite direction show a negative correlation. Vectors crossing at right angles indicate independency of both parameters. The absence of collinearity between selected parameters was then checked, as well as the significance of the constrained analysis.